OPEN ACCESS

ORIGINAL RESEARCH

ATR-16 syndrome: mechanisms linking monosomy to phenotype

Christian Babbs ,[1] Jill Brown,[1] Sharon W Horsley,[1] Joanne Slater,[1] Evie Maifoshie,[1] Shiwangini Kumar,[2] Paul Ooijevaar,[3] Marjolein Kriek,[3] Amanda Dixon-McIver,[2] Cornelis L Harteveld,[3] Jan Traeger-Synodinos,[4] Andrew O M Wilkie,[5,6] Douglas R Higgs,[1] Veronica J Buckle[1]

► Additional material is published online only. To view, please visit the journal online (http://dx.doi.org/10.1136/jmedgenet-2019-106528).

[1]MRC Molecular Haematology Unit, MRC Weatherall Institute of Molecular Medicine, University of Oxford, Oxford, UK
[2]IGENZ Ltd, Auckland, New Zealand
[3]Department of Clinical Genetics, Leiden University Medical Center, Leiden, The Netherlands
[4]Department of Medical Genetics, National and Kapodistrian University of Athens, Athens, Greece
[5]Clinical Genetics Group, MRC Weatherall Institute of Molecular Medicine, University of Oxford, Oxford, UK
[6]Craniofacial Unit, Oxford University Hospitals NHS Trust, John Radcliffe Hospital, Oxford, UK

Correspondence to
Dr Christian Babbs and Professor Veronica J Buckle, MRC MHU, MRC WIMM, University of Oxford, Oxford, UK; christian.babbs@imm.ox.ac.uk, veronica.buckle@imm.ox.ac.uk

Received 28 August 2019
Revised 29 November 2019
Accepted 5 December 2019
Published Online First 31 January 2020

Check for updates

© Author(s) (or their employer(s)) 2020. Re-use permitted under CC BY. Published by BMJ.

To cite: Babbs C, Brown J, Horsley SW, *et al*. *J Med Genet* 2020;**57**:414–421.

ABSTRACT

Background Deletions removing 100s–1000s kb of DNA, and variable numbers of poorly characterised genes, are often found in patients with a wide range of developmental abnormalities. In such cases, understanding the contribution of the deletion to an individual's clinical phenotype is challenging.

Methods Here, as an example of this common phenomenon, we analysed 41 patients with simple deletions of ~177 to ~2000 kb affecting one allele of the well-characterised, gene dense, distal region of chromosome 16 (16p13.3), referred to as ATR-16 syndrome. We characterised deletion extents and screened for genetic background effects, telomere position effect and compensatory upregulation of hemizygous genes.

Results We find the risk of developmental and neurological abnormalities arises from much smaller distal chromosome 16 deletions (~400 kb) than previously reported. Beyond this, the severity of ATR-16 syndrome increases with deletion size, but there is no evidence that critical regions determine the developmental abnormalities associated with this disorder. Surprisingly, we find no evidence of telomere position effect or compensatory upregulation of hemizygous genes; however, genetic background effects substantially modify phenotypic abnormalities.

Conclusions Using ATR-16 as a general model of disorders caused by CNVs, we show the degree to which individuals with contiguous gene syndromes are affected is not simply related to the number of genes deleted but depends on their genetic background. We also show there is no critical region defining the degree of phenotypic abnormalities in ATR-16 syndrome and this has important implications for genetic counselling.

INTRODUCTION

Cytogenetic, molecular genetic and more recently, next-generation sequencing (NGS) approaches have revealed CNVs in the human genome ranging from 1 to 1000s of kilobases (kb).[1 2] CNVs are common in normal individuals and have been identified in ~35% of the human genome.[1] When present as hemizygous events, in phenotypically 'normal' individuals, these imbalances are considered benign; however, CNVs are also among the most common causes of human genetic disease and they have been associated with a wide range of developmental disabilities present in up to 14% of the population.[3]

CNVs have been shown to play an important role in neurodevelopmental disorders including autism spectrum disorder, bipolar disorder and schizophrenia as well as influencing broader manifestations such as learning disabilities, abnormal physical characteristics and seizures.[4] Some CNVs occur recurrently in association with one particular phenotype: for example, deletions within 16p11.2 and/or chromosome 22q are frequently associated with autism, and deletions within 15q13.3 and 1q21.1 are found in schizophrenia. However, the impact of most CNVs on phenotype is much less clear.[4] Difficulty in interpreting CNVs particularly occurs when they result from complex rearrangements such as those associated with unbalanced translocations, inversions and imprinting effects.

To understand the principles and mechanisms by which CNVs lead to developmental abnormalities we have simplified the issue by studying the relationship between uncomplicated deletions within the region ~0.3 to ~2 Mb in the subtelomeric region of chromosome 16 and the resulting phenotypes. The 41 individuals studied here (comprising 12 new and 29 previously reported cases) represent a cohort of patients with the α-thalassaemia mental retardation (MR) contiguous gene syndrome, involving the chromosomal region 16p13.3, termed ATR-16 syndrome (MIM 141750).[5]

Individuals studied here have monosomy for various extents of the gene-rich distal region at 16p13.3 and all individuals with ATR-16 syndrome have α-thalassaemia because two of the four paralogous α-globin genes are deleted (--/αα) and this manifests as mild hypochromic microcytic anaemia. In combination with a common small deletion involving one α-gene on the non-paralogous allele (--/-α), patients may have a more severe form of α-thlassaemia referred to as HbH disease.[6] Some patients also have MR, developmental abnormalities and/or speech delay and facial dysmorphism. The most severe cases also manifest abnormalities of the axial skeleton. By precisely defining the 16p13.3 deletions in 11 cases (with a further 8 characterised by microarray) we address whether the associated neurological and developmental defects are simply related to the size of the deletions and the number of genes removed and whether there are critical haploinsufficient genes within this region. Our

J Med Genet: first published as 10.1136/jmedgenet-2019-106528 on 31 January 2020. Downloaded from http://jmg.bmj.com/ on April 23, 2024 by guest. Protected by copyright.

findings suggest that while the loss of an increased number of genes tends to underlie more severe phenotypic abnormalities, the genetic background in which these deletions occur contributes to the occurrence of MR and developmental abnormalities.

Finally, this subgroup of ATR-16 patients also allowed us to address two long-standing questions associated with large subcytogenetic deletions: those of compensatory gene expression and telomere proximity effect (TPE) in cases of telomere repaired chromosomal breakages.

METHODS

Patients

Here, we focus on a cohort of patients with pure monosomy within 16p13.3 to clarify the effect of the deletion. In this work, we identify or refine the breakpoints of 14 deletions in a total of 19 individuals (including 9 cases from 4 families designated TN, TY, CS and SH and 10 singleton cases (OY, LA, YA, BA, NL, CJ, MY, BAR, IM and LIN)). In addition, we review 11 cases from 2 families (designated BF and F) and 11 singleton cases (JT, CV, AB, GZ, GIB, DO, SCH, PV, FT, BO, HN). Together this amounts to 20 familial cases from 5 pedigrees and 21 singletons amounting to a total of 41 patients.

Fluorescent in situ hybridisation

FISH studies were carried out on fixed chromosome preparations as previously described[7] from each patient using a series of cosmids covering the terminal 2 Mb of chromosome 16p (online supplementary table 1). FISH studies were also performed using probes specific for the subtelomeric regions of each chromosome in order to exclude any cryptic chromosomal rearrangements. Subtelomeric rearrangements were detected as previously described.[8 9]

Southern blotting

Single copy probes labelled with α^{32}P-dCTP were synthesised and used to hybridise Southern blots of DNA isolated from transformed lymphoblastoid cells.

PCR detection of chromosomal deletions

DNA was extracted from mouse/human hybrid cell lines or transformed lymphoblastoid lines. Based on FISH results with chromosome 16 cosmids, primer pairs were designed located at regular intervals across the breakpoint clone. To refine the 16p breakpoint, PCR amplification was performed using normal and abnormal patient hybrid DNA obtained from mouse erythroleukaemia (MEL cells) fused to patient cells and selected to contain a single copy of human chromosome 16 generated as previously described[10] as template. A positive PCR indicated the sequence was present; a negative PCR indicated it was deleted.

Telomere-anchored PCR amplification

Telomere-anchored PCR was undertaken using a primer containing canonical telomeric repeats in conjunction with a reverse primer specific for the normal 16p sequence (primer sequences provided in online supplementary table 2). Telomere repeat primers hybridise at any location in telomere repeats so heterogeneous amplification products are produced. Amplification products were purified and digested with restriction endonucleases BamHI or EcoRI and products ligated into appropriately prepared pBluescript. Resulting colonies were screened for inserts and DNA Sanger sequenced.

Quantification of gene expression

Total RNA was isolated from Epstein-Barr virus transformed lymphoblastoid cell lines for 11 patients (OY, TY, BA, MY, BO, CJ, YA, TN (Pa), SH (Pa), LIN and IM) and 20 control individuals using TRI reagent. In the case of OY, the genes *MRPL28*, *TMEM8*, *NME4*, *DECR2* and *RAB11FIP3* were excluded from the analysis as they are proximal to the deleted region and are not hemizygous in this patient. In the case of CJ, *POLR3K*, *C16ORF33*, *MPG* and *C16ORF35* are excluded as they are distal to the interstitial deletion in this patient. cDNA synthesis was performed with the AffinityScript kit (Stratagene). Where gene expression was measured by quantitative real-time PCR, TaqMan Gene Expression Assays Applied Biosystems (ABI, www.appliedbiosystems.com) were used. Genes and assay numbers are given in online supplementary information.

Microarray analysis

Details of the microarray platforms used for each patient are given in online supplementary information.

Whole genome sequencing

Whole genome sequencing (WGS) was carried out, using DNA from the three affected members of the TN family and YA, at Edinburgh Genomics, The University of Edinburgh. The pathogenicity of each variant was given a custom deleterious score based on a six-point scale,[11] calculated using output from ANNOVAR.[12] This was used to prioritise variants present in the hemizygous region of chr16p13.3 in each patient and also genome-wide.

RESULTS

Clinical features of ATR-16 syndrome

In addition to the α-thalassaemia, manifesting as a microcytic anaemia (identified by full blood count) that is always present, common features of ATR-16 syndrome include speech delay, developmental delay and a variable degree of facial dysmorphism and, in severe cases, abnormalities of the axial skeleton. Individual case reports are provided in online supplementary information; newly cloned breakpoint sequences are shown in figure 1; deletions are shown in figure 2 and phenotypic abnormalities are summarised in table 1. Deletions larger than 2000 kb including the *PKD1* and *TSC2* genes lead to severe MR with polycystic kidney disease and tuberous sclerosis, respectively.[13]

Twelve individuals from 9 pedigrees are reported here for the first time (OY, CS, CS (father), LA, TY (MI), TY (Mi), YA, SH (P), SH (Ju), CJ, MY and BAR) and we refine or identify the breakpoints in five previously reported cases (BA, TN, IM, NL, LIN). We define breakpoints at the DNA sequence level in 7 of the 14 pedigrees studied (figure 1), 6 of which have been repaired by the addition of a telomere or subtelomere. In the remaining family (SH), the deletion is interstitial and mediated by repeats termed short interspersed nuclear elements.

Identification of co-inherited deleterious loci

Six individuals from four families (LA, BA, YA and TN) have 16p13.3 deletions smaller than 1 Mb and yet show relatively severe abnormalities. To test whether 16p13.3 deletions of <1 Mb may be unmasking deleterious mutations on the intact chromosome 16 allele in severely affected patients, we performed WGS where DNA was available (YA and the three affected members of the TN family) and considered only coding variants in the hemizygous region of chromosome 16. However, only common variants (allele frequency >5%) were present (online supplementary

J Med Genet: first published as 10.1136/jmedgenet-2019-106528 on 31 January 2020. Downloaded from http://jmg.bmj.com/ on April 23, 2024 by guest. Protected by copyright.

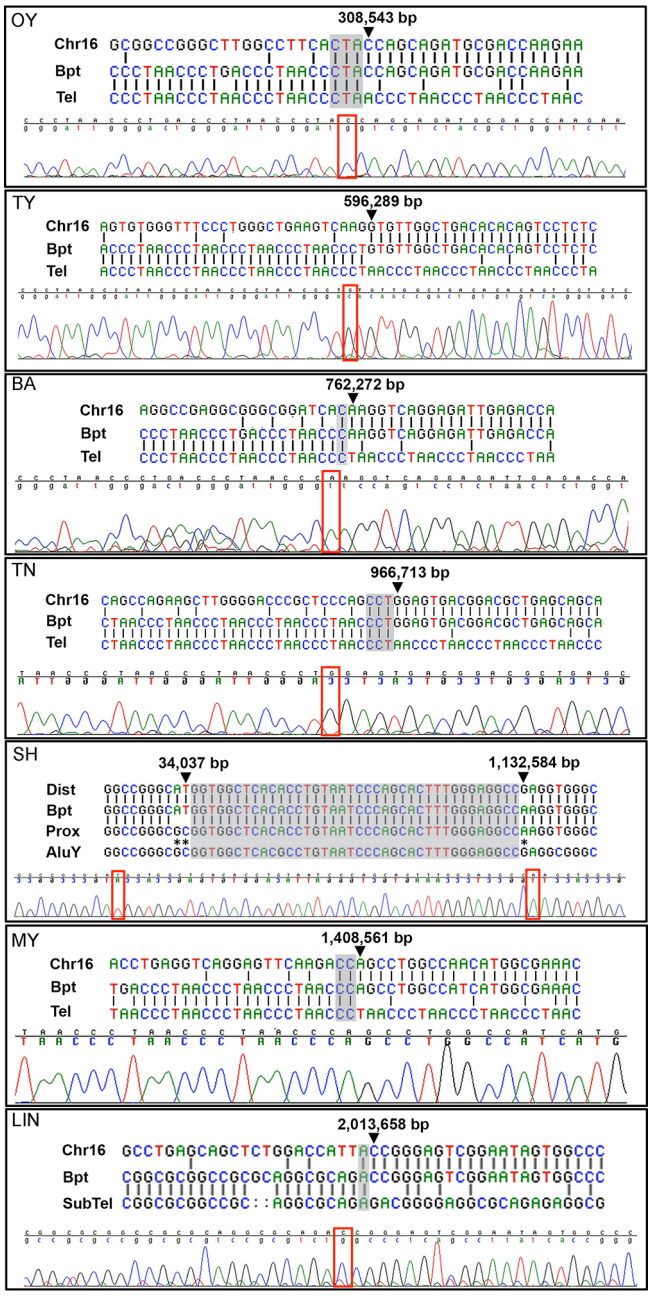

Figure 1 Chromosome 16 breakpoint sequences. DNA sequences at ATR-16 breakpoints. Patient codes are given in the upper left of each panel. For each case, alignment of the two normal sequences is shown with sequence from the derivative chromosome (upper) with chromatogram traces traversing each breakpoint (lower). Areas of ambiguity are highlighted with grey boxes and the location of the last unambiguous base pair(s) are denoted by arrowheads and red boxes. Chr16, normal chromosome 16 sequence; Bpt, breakpoint sequence; Tel, telomere repeat sequence; SubTel, subtelomere repeat sequence; Prox, proximal chromosome 16 sequence; Dist, distal chromosome 16 sequence; AluY, AluY repetitive element. Asterisks indicate informative polymorphisms allowing sequence origins to be identified. For patients MY and OY, a telomere primer with a mismatched G nucleotide was used.

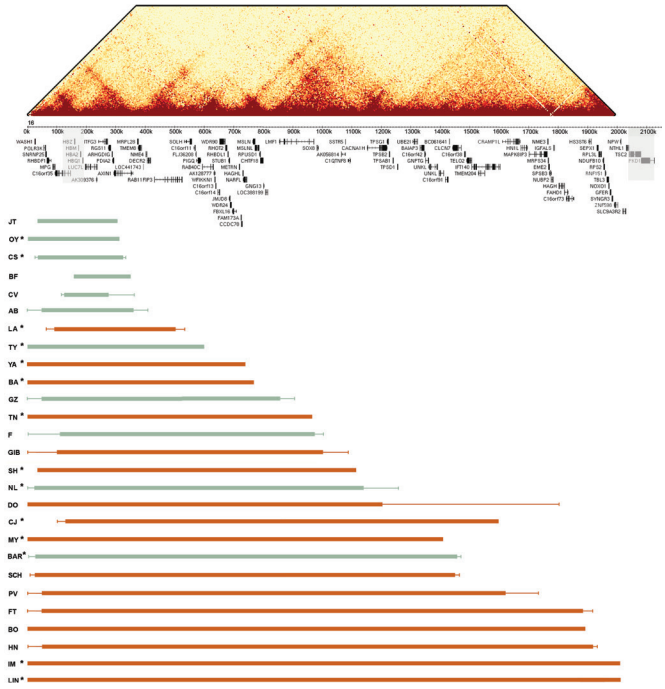

Figure 2 Summary of ATR-16 deletions. Upper: HiC interaction map showing interactions across the terminal 2 Mb of chromosome 16 at a 5 kb resolution in K562 cells (data from Rao *et al*[40]). This shows how the ATR-16 deletions detailed in the lower section may impact the genome organisation. Middle: the positions of the α-globin cluster and other genes within this region are indicated. The α-globin genes and genes that, when mutated, are associated with tuberous sclerosis and adult polycystic kidney disease are shown in shaded boxes. Lower: the extent of each deletion is shown with the patient code (left). Deletions shown in green cause no other abnormalities apart from α-thalassaemia and those in red cause at least one other abnormality present in ATR-16. Solid bars indicate regions known to be deleted and fine lines show regions of uncertainty. Asterisks indicate individuals whose deletion breakpoints have been cloned or refined in this work.

table 3) suggesting the cause(s) of the relatively severe phenotypes in these patients reside elsewhere in the genome. To identity rare variants genome-wide, we considered only those absent from the publicly available databases. This analysis yielded 14 variants shared between the three affected individuals of family TN (online supplementary table 4). Of these, only one (chr15:64 782 684 G>A) affects a gene possibly involved in the broader ATR-16 phenotypic abnormalities. This change leads to a R12X nonsense mutation in *SMAD6*, a negative regulator of the bone morphogenetic protein signalling pathway. Heterozygous mutations in *SMAD6* have been reported to underlie craniosynostosis, speech delay, global developmental delay, fine motor impairment and aortic valve abnormalities with variable penetrance (see 'Discussion' section). We checked inheritance of the *SMAD6* R12X variant in members of the TN family where samples were available and found it most likely came from the unaffected grandmother (individual I,2 in online supplementary figure 4). A phenotypically normal elder sister also inherited this variant. These findings suggest that coinheritance of this *SMAD6* loss of function variant with the chromosome 16 deletion may lead to the increased severity of the ATR-16 syndrome.

Further evidence that the effect of ATR-16 deletions is modified by other loci comes from patients SH (Ju) and SH (Pa), who harbour the same chromosome 16 deletion. Patient SH (Pa) has developmental delay and skeletal abnormalities, however, his mother SH (Ju) does not have craniofacial nor skeletal abnormalities nor developmental delay, although she suffers from severe anxiety and depression (see figures 1 and 2 and online supplementary information). Genome-wide microarray analysis

J Med Genet: first published as 10.1136/jmedgenet-2019-106528 on 31 January 2020. Downloaded from http://jmg.bmj.com/ on April 23, 2024 by guest. Protected by copyright.

Table 1 ATR-16 syndrome phenotypic severity

Case*	Sex	Deletion coordinates (hg18)	Methods	Origin	Mechanism	MR	AT	SD	DD	FD	SA	Reference(s)
JT	F	34,113 bp to 301,556 bp†	F,SB,S	Mat	De novo	–	+	–	–	–	–	Horsley, 2001[9]
OY‡	F	0 bp to 308,540 bp	F,SB,S	Pat	De novo	–	+	–	–	–	–	This study
CS‡(+1)§	F	~36,766 bp to 328,247 bp	A	Pat	Inherited	–	+	–	–	–	–	This study
BF (+5)§	M	166,680 bp to 342,681 bp	WGS	na	De novo	–	+	–	–	–	–	Heireman *etal*[24]
CV	F	~1 22 000 bp to 2 99 000–3 75 000 bp	M	na	na	–	+	–	–	–	–	Coelho *etal*[41]
AB	na	0–45,799 bp to 3 50 916–4 00 279 bp	M	na	na	–	+	–	–	–	–	Harteveld *etal*[42]
LA‡	M	~94,214bp to 502,227 bp	A	Pat	Inherited	–	+	+	+/-	–	–	This study
TY(MI)‡	M	0 bp to 596,289 bp	F,SB,S	na	na	–	+	–	–	–	–	This study
TY(Mi)‡	F	0 bp to 596,289 bp	F,SB,S	Pat	Inherited	–	+	–	–	–	–	This study
YA‡	F	0 bp to 747,840 bp	F,A	na	na	na	+	+	+	+	–	This study
BA‡	F	0 bp to 762,370 bp	F,SB,S	Pat	De novo	–	+	–	+	–	–	Daniels *etal*[43]
GZ	M	0–45,799 bp to 8 69 698–9 00 907 bp	M	Mat	Inherited		+	–	–	–	–	Harteveld *etal*[18]
TN(Pa)‡	F	0 bp to 966,710 bp	F,SB,S	Mat	De novo	+/-	+	+	+	+	–	Daniels *etal*[43]
TN(Pe)‡	M	0 bp to 966,710 bp	F,SB,S	Mat	Inherited	+	+	+	+	+	–	Daniels *etal*[43]
TN(Al)‡	M	0 bp to 966,710 bp	F,SB,S	Mat	Inherited	+	+	+	+	+	–	Daniels *etal*[43]
FI.2	F	0–45,799 bp to~9 76 591 bp	M	na	na	–	+	–	–	–	–	Bezerra *etal*[20]
FII.1	M	0–45,799 bp to~9 76 591 bp	M	Mat	Inherited	–	+	–	–	–	–	Bezerra *etal*[20]
FII.2	M	0–45,799 bp to~9 76 591 bp	M	Mat	Inherited	–	+	–	–	–	–	Bezerra *etal*[20]
FII.4	F	0–45,799 bp to~9 76 591 bp	M	Mat	Inherited	–	+	–	–	–	–	Bezerra *etal*[20]
FIII.1	M	0–45,799 bp to~9 76 591 bp	M	Mat	Inherited	–	+	–	–	–	–	Bezerra *etal*[20]
GIB	F	~1 00 000 bp to~1,000,000 bp	F,A	na	De novo	+	+	+	+	+	–	Gibson, 2008[44]
SH(Pa)‡¶	M	34,037 bp to 1,132,584 bp	F,SB,S	Mat	Inherited	+	+	na	+	+	+	This study
SH(Ju)‡¶	F	34,037 bp to 1,132,584 bp	F,SB,S	na	na	–	+	na	–	–	–	This study
NL‡	M	0–23 949 bp to~1,246,849 bp	A,M	na	De novo	–	+	–	–	–	–	Phylipsen *etal*[45] ; This study
DO	F	0 bp to 1,175,000–1,805,487 bp	SB	Mat	Unknown	+	+	+	+	+	–	Wilkie *etal*[5]
CJ‡	M	120,000 bp to 1,357,000 bp	F,A	Mat	De novo	+	+	+	+	+	+	This study
MY‡	F	0 bp to 1,408,950 bp	F,SB,S	Mat	De novo	+	+	+	+	+	–	This study
BAR‡	M	0–23,949 bp to~1,440,000 bp	A,M	na	De novo	–	+	–	–	–	–	This study
SCH	M	~281,65 bp to 1,447,989 bp	F,A,M	na	De novo	+	+	+	+	+	+	Scheps *etal*[28]
PV	M	0–45,799 bp to 1,615,979–1,730,426 bp	M	na	De novo	+	+	+	+	+	+	Harteveld *etal*[18]
FT	F	0–45,799 bp to 1,880,277–1,913,866 bp	M	na	De novo	+	+	+	+	+	+	Harteveld *etal*[18]
BO	M	0 bp to 1,886,763 bp	C,F,SB, S	Pat	De novo	+	+	na	+	+	+	Wilkie *etal*[5] ; Lamb *etal*[46] ; Daniels *etal*[43]
HN	M	0–45,799 bp to 1,913,923–1,928,982 bp	M	na	De novo	+	+	+	+	+	+	Harteveld *etal*, 2007[18]
IM‡	F	0 bp to 2,011,646 bp	F,SB,A	na	na	+	+	–	+	+/-	+	Felice [47] ; Fei *etal*[48] ; Daniels *etal*[43]
LIN‡	F	0 bp to 2,013,657 bp	F,SB,S	Pat	De novo	+	+	+	+	+	–	Lindor *etal*[49] ; Daniels *etal*[43]

+ indicates presence of an abnormality; – indicates absence and +/– indicates borderline assessment.
Methods column summarises the methods used to refine or identify the breakpoint:C, cytogenetics; F, FISH; WGS, Whole Genome Sequencing; M, MLPA; SB, Southern blot; A, microarray, S, breakpoint has been DNA sequenced.
*ATR-16 individuals are identified by unique codes, references are shown in figure 2. Pale green rows indicate ATR-16 individuals with only alpha-thalassemia, yellow rows indicate ATR-16 individuals also have at least one other abnormality but no defects of the axial skeleton and orange rows indicate the individual also has skeletal defects.
†40 bp ambiguity, values taken from midpoint
‡Indicates individuals whose deletion breakpoints have been cloned or refined in this work.
§There numbers refer to other family members who carry this deletion and have no associated abnormalities apart from alpha-thalassemia
¶Individuals have discordant abnormalities, most likely due to a deletion in *NRXN1*.
A, microarray; AT, alpha-thalassaemia; C, cytogenetics; DD, developmental delay; F, FISH; FD, facial dysmorphism; M, Multiplex Ligation-dependent Probe Amplification (MLPA); MR, mental retardation; na, data not available; S, breakpoint has been DNA sequenced; SA, skeletal abnormalities; SB, Southern blot; SD, speech delay; WGS, whole genome sequencing.

revealed that both SH (Ju) and SH (Pa) harbour a ~133 kb deletion on the short arm of chromosome 2 including exons 5–13 of *NRXN1* (online supplementary figure 1).

Chromatin structure

Recent reports demonstrate chromosomal rearrangements, including deletions, can result in aberrant DNA domain topology and illegitimate enhancer-promoter contact causing gene misexpression.[14] Chromatin contact frequency is shown for the terminal 2 Mb of chromosome 16 in figure 2 to illustrate the effect of the deletions reported here on the chromatin structure. The deletion in BA removes ~50% of the self-interacting domain in which *CHTF18*, *RPUSD1*, *GNG13* and *LOC388199* reside, thereby potentially removing *cis*-acting regulatory elements of these genes, although the genes themselves remain intact. In the case of CJ, the deletion brings the powerful α-globin enhancer cluster[15] into proximity of *CRAMP1L* and may cause its aberrant expression in developing erythroblasts. Although topologically associating domains have been reported to be stable structures,[14] many chromatin contacts are now known to vary in a tissue-specific fashion[16] and therefore it is not possible to predict which genes may be aberrantly expressed in any given tissue as a result of the ATR-16 deletions.

J Med Genet: first published as 10.1136/jmedgenet-2019-106528 on 31 January 2020. Downloaded from http://jmg.bmj.com/ on April 23, 2024 by guest. Protected by copyright.

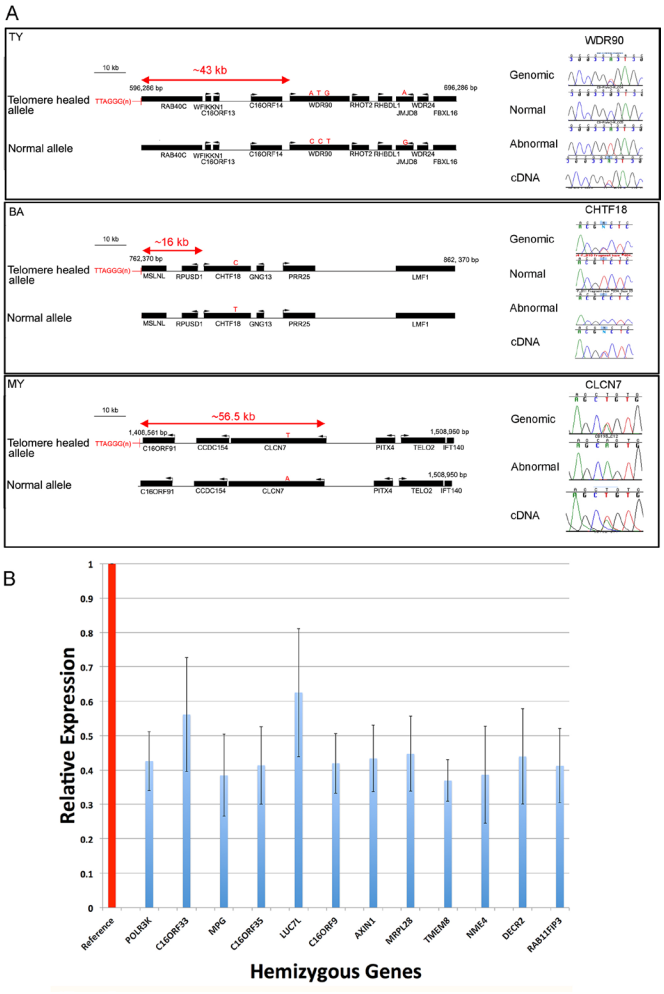

Figure 3 Effect of breakpoints and deletions on gene expression. (A) Schematic view of breakpoint positions in three patients with nearby expressed polymorphic genes. Genes are represented by black bars and transcription direction is indicated by an arrow. Polymorphic bases are shown by red letters indicating variant alleles and the distance of the promoter of each measured gene from the breakpoint is shown. On the right of each panel chromatograms show the quantity of the allele present in genomic DNA and cDNA from patient lymphoblastoid cells. (B) Expression of 12 genes within 500 kb of the tip of the short arm of chromosome 16 in lymphoblastoid cells from 20 normal individuals, shown as reference (red column) and from 11 ATR-16 individuals hemizygous for each gene. Measurements in control cells are normalised to 1 (red column), relative expression in ATR-16 patient cells is shown in blue. Error bars show SD. Gene expression was measured in triplicate and data combined.

Compensatory gene expression

One explanation for the relatively mild abnormalities in many cases of ATR-16 syndrome with deletions up to 900 kb may be compensatory transcriptional upregulation of the homologues of deleted genes on the undamaged chromosome 16. This has been described as part of the mechanism of genetic compensation, also termed genetic robustness.[17] To assay for compensatory gene transcription, we used qPCR to measure expression of 12 genes within the terminal 500 kb of chromosome 16 in lymphoblastoid cells from 20 normal individuals and from 11 patients with monosomy for the short-arm of chromosome 16 and found no evidence of compensatory upregulation: transcripts of all deleted genes were present at ~50% of the normal levels in these cells (figure 3B). It is possible that other genes in downstream pathways affected by haploinsufficiency may be transcriptionally upregulated, however, the mechanisms underlying this are complex and beyond the scope of this study.

Telomere position effect

To determine the effect of telomere proximity on genes adjacent to telomere-healed breakpoints, we measured their expression relative to the allele present in a normal chromosomal context. To achieve this, we screened them for informative SNPs in EBV transformed lymphoblastoid cells generated from ATR-16 patients. The phase of polymorphisms was established using MEL cells fused to patient cells and selected to contain a single copy of human chromosome 16, generated as previously described.[10] Expressed coding polymorphisms were present in genes whose promoters are <60 kb away from breakpoints in three patients: TY, MY and BA.

For TY, the nearest gene expressed in lymphoblastoid cells containing a coding polymorphism is *WDR90*, the promoter of which is ~43.1 kb from the abnormally appended telomere (figure 3A). For BA, *CHTF18* is the closest expressed polymorphic gene with the promoter ~16.3 kb away from the breakpoint. For MY, *CLCN7* is the closest gene expressed in lymphoblastoid cells to contain a polymorphism, the promoter of this gene is ~56.1 kb away from the telomere stabilised lesion. To determine whether either allele of each of these three genes is silenced we prepared genomic DNA and cDNA from each cell sample and Sanger sequenced amplified fragments containing informative polymorphisms. We compared peak heights of polymorphic bases in chromatograms derived from cDNA and genomic DNA. None of the alleles assayed in the three patients tested showed any evidence of a repressive effect (figure 3A).

DISCUSSION

We characterised deletions leading to simple monosomy of the short arm of chromosome 16 that cause ATR-16 syndrome. Many ATR-16 patients suffer from neurodevelopmental abnormalities and one of the main questions in this disease, and in the study of CNVs in general, is how deletion size relates to phenotypic abnormalities. The monosomies analysed here show the likelihood and severity of neurological and developmental abnormalities increases with deletion size, however, there is no clear correlation.

The deletions in patients reported and reviewed here range from ~0.177 to ~2 Mb. Previous studies suggest the critical region leading to abnormalities in addition to α-thalassaemia is an 800 kb region between ~0.9 and~1.7 Mb from the telomere of chromosome 16p[18] and *SOX8* has been proposed as the critical haploinsufficient gene.[19] However, a report of a family with no developmental delay nor MR harbouring a 0.976 Mb deletion, suggests deletions of *SOX8* may not lead to MR with complete penetrance and any 'critical region' for MR must start after this point[20] (family 'F' in figure 2 and table 1). Supporting this we report patients NL and BAR, who have deletions of ~1.14 and ~1.44 Mb, respectively and show no abnormalities beyond α-thalassaemia.

By contrast, we find LA (deletion ~408 kb) has speech delay and YA (deletion ~748 kb) has speech and developmental delay and facial dysmorphism (figure 2, table 1). Family members of YA also have omphalocele, umbilical hernia and pyloric stenosis suggesting there are other loci rendering YA susceptible to developmental abnormalities. BA (deletion ~762 kb), who has a similarly sized deletion to YA, has developmental delay but no other abnormalities. Three other patients with deletions <1 Mb (TN

J Med Genet: first published as 10.1136/jmedgenet-2019-106528 on 31 January 2020. Downloaded from http://jmg.bmj.com/ on April 23, 2024 by guest. Protected by copyright.

(Pa), TN (Pe) and TN (Al)) have speech delay and facial dysmorphism. This suggests the risk of developmental and neurological abnormalities arises from much smaller terminal chromosome 16 deletions (~400 kb) than previously reported.

In family SH, we have identified a strong candidate for the discordant abnormalities: deletion of *NRXN1*. *NRXN1* encodes a cell surface receptor involved in the formation of synaptic contacts and has been implicated in autism spectrum disorder, facial dysmorphism, anxiety and depression, developmental delay and speech delay.[21] There is a higher incidence of autism in males than in females, with a ratio of 3.5 or 4.0 to 1.[22] This phenomenon is also specifically found in individuals with autism resulting from rearrangements of *NRXN1*[23], where two affected siblings inherited a deletion of *NRXN1* from their unaffected mother. It is therefore possible SH (Ju) is protected by her gender from the effects of *NRXN1* disruption while the neurological and skeletal abnormalities in SH (Pa) arise from the complex interaction of *NRXN1* perturbation with his gender and coinheritance of the 16p13.3 deletion. Abnormalities in siblings of YA and BF[24] also suggest there may be other predisposing genes. Such loci compromise genetic robustness proposed to minimise the effect of deletions and loss of function mutations.[17] Another example is the *SMAD6* R12X nonsense mutation present in all three affected members of family TN. Some patients with loss of function mutations in *SMAD6* have neurological abnormalities[25] while others have not,[26] suggesting variable penetrance. Our analysis shows there are no likely pathogenic variants on the hemizygous region of chromosome 16 in TN, suggesting modifying loci are present elsewhere in the genome. These may be rare variants (such as those identified in the TN and SH families) or common variation; a recent study shows that common genetic variants (allele frequency >5% in the general population) contribute 7.7% of the variance of risk to neurodevelopmental disorders,[27] highlighting the complexity of this area.

Together these observations suggest that monosomy for 16p13.3 unmasks the effects of other variants genome-wide. This is supported by findings in SCH who has a very similar deletion to BAR and is more severely affected possibly owing to the presence of other CNVs.[28] At the other end of the spectrum, large ATR-16 deletions may be associated with relatively mild abnormalities. In LIN (16p13.3 deletion ~2000 kb), there are no abnormalities of the axial skeleton and very mild facial dysmorphism. Similarly, in the case of IM (deletion size ~2000 kb), facial abnormalities are very mild and there is no evidence of language delay. Here, we propose chromosome 16p13.3 deletions larger than 400 kb predispose to MR and associated developmental abnormalities, however, we find no evidence for critical regions that incrementally worsen ATR-16 syndrome abnormalities.

In this work, we were able to provide evidence that CNVs and other variation genome-wide is likely to impact ATR-16 severity. However, we would not recommend this approach is yet widely applied as the impact of novel CNVs and sequence variants is challenging to interpret, especially when co-inherited with a terminal chromosome 16 deletion. We were unable to expand genome-wide analyses beyond the six patients (SH (Pa), SH (Ju), TN (Pa), TN (Pe), TN (Al) and YA) studied by microarray or WGS here and so cannot exclude the possibility variation genome-wide may influence the presentation of other ATR-16 patients reported and reviewed here. Previous work in human cells has shown that telomeres may affect chromatin interactions at distances of up to 10 Mb away from the chromosome ends[29] reducing expression of the intervening genes. This phenomenon, termed TPE, is thought to be mediated by the spreading of telomeric heterochromatin to silence nearby genes. In budding yeast, this effect can extend a few kb towards the subtelomeres, although in some cases yeast telomeres can loop over longer distances[30] and repress genes up to 20 kb away from the end of the chromosome. However, we could not detect compensatory upregulation of the homologues of deleted genes. Recently, a case of ATR-16 was reported with a~948 kb deletion who presented with a neuroblastoma in utero.[31] These authors speculate that haploinsufficiency of the tumour suppressor *AXIN1* may have contributed to the neuroblastoma. Our finding that the remaining *AXIN1* allele shows no compensatory expression supports this hypothesis.

Terminal chromosome deletions are the most common subtelomeric abnormalities.[32] The 16p deletions reported here are among the most common terminal deletions along with 1p36 deletion syndrome, 4p terminal deletion (causing Wolf-Hirschhorn syndrome), 5p terminal deletions (causing Cri-du-chat syndrome), 9q34 deletion syndrome and 22q terminal deletion syndrome. Despite their impact on human health, the mechanisms and timing underlying telomeric breakage remain unknown. Findings of terminal deletions of 16p reported and reviewed here and smaller deletions previously reported by our laboratory[33] compared with more complex rearrangements at 1p, 22q and 9qter implies different chromosomes are predisposed to different breakage and rescue mechanisms. ATR-16 deletions are equally likely to have arisen on the maternal or paternal chromosome. There is no evidence that the parental origin affects the phenotypic severity of the ATR-16 syndrome, suggesting imprinting does not play a role in ATR-16 pathogenesis.

The presence of high and low copy number repeats at breakpoints may play a role in stimulating the formation of non-recurrent breakpoints.[34] Low copy repeats (LCRs) are also mediators of non-allelic homologous recombination[35] and could be involved in chromosome instability leading to terminal deletion. Following breakage, chromosomes can acquire a telomere by capture or de novo telomere addition, which is thought to be mediated by telomerase and this is stimulated by the presence of a telomeric repeat sequence to which the RNA subunit of telomerase can bind.[36] We found 5 out of 6 telomere healed events share microhomology with appended telomeric sequence. This is the same ratio (5 out of 6 breakpoints with microhomology) described by Flint *et al* and supported by Lamb *et al* (1 out of 1) giving a total 11 out of 13 reported telomere-healed breaks characterised on 16p13.3 share microhomology with appended telomere sequences, strongly suggesting a role for internal telomerase binding sites.[37] It may also be that telomerase binding to internal binding sites may inappropriately add telomeres and thereby contribute to the generation of the breakpoints.

The lack of evidence for TPE in silencing gene expression is surprising and at variance with previous findings,[38] which show that TPE can influence gene expression at least 80 kb from the start of telomeric repeats. However, TPE is likely to be context and cell type dependent. Additionally, because of the lack of informative expressed polymorphisms in the patients studied here it was not possible for us to assay expression of genes immediately adjacent to telomeres and a more comprehensive screen may reveal TPE-mediated gene silencing closer to the telomere. Additionally, when the area of chromatin interaction (visualised by HiC) is considered (figure 2), contact domains for many genes adjacent to chromosomal breaks are severely disrupted. This is likely to include the loss of *cis*-acting regulatory elements and may bring the genes under the control of illegitimate regulatory elements.[39] Therefore, it is likely that genes adjacent to breakpoints would be incorrectly spatiotemporally expressed.

J Med Genet: first published as 10.1136/jmedgenet-2019-106528 on 31 January 2020. Downloaded from http://jmg.bmj.com/ on April 23, 2024 by guest. Protected by copyright.

This work substantially increases the number of fully characterised cases of ATR-16 syndrome reported and provides a uniquely well-characterised model for understanding how sporadic deletions giving rise to extended regions of monosomy may affect phenotype. The findings show larger deletions have a greater impact, but importantly our analysis suggesting there is no critical region defining the degree of phenotypic abnormalities has important implications for genetic counselling. Analysis of patients with uncomplicated deletions also revealed unexpected background genetic effects that alter phenotypic severity of CNVs.

Acknowledgements The authors would like to thank Markissia Karagiorga-Lagana, MD, ex Director, Thalassaemia Unit, 'Aghia Sophia' Children's Hosital, Athens, Greece for referring case BAR.

Contributors DRH and VJB conceived the project. CB, VJB and DRH wrote the paper. CB, JS, CLH, JB, EM, SWH, VJB, SK and AD-M performed experimental work. JT-S, PO, MK, AD-M and AOMW assessed patients and clinical data. All authors commented on the manuscript.

Funding This work was supported by the Medical Research Council grant number: (MC_uu_12009).

Competing interests None declared.

Patient consent for publication Not required.

Ethics approval This study was approved by the NRES Committee North West, Haydock, HRA NRES Centre, Manchester under the title 'Establishing the molecular basis for atypical forms of thalassaemia' (reference number MREC: 03/8/097) with written consent from patients and/or parents.

Provenance and peer review Not commissioned; externally peer reviewed.

Data availability statement All data relevant to the study are included in the article or uploaded as supplementary information.

Open access This is an open access article distributed in accordance with the Creative Commons Attribution 4.0 Unported (CC BY 4.0) license, which permits others to copy, redistribute, remix, transform and build upon this work for any purpose, provided the original work is properly cited, a link to the licence is given, and indication of whether changes were made. See: https://creativecommons.org/licenses/by/4.0/.

ORCID iD

Christian Babbs http://orcid.org/0000-0002-1898-5878

REFERENCES

1 Iafrate AJ, Feuk L, Rivera MN, Listewnik ML, Donahoe PK, Qi Y, Scherer SW, Lee C. Detection of large-scale variation in the human genome. *Nat Genet* 2004;36:949–51.
2 MacDonald JR, Ziman R, Yuen RKC, Feuk L, Scherer SW. The database of genomic variants: a curated collection of structural variation in the human genome. *Nucleic Acids Res* 2014;42:D986–92.
3 Kaminsky EB, Kaul V, Paschall J, Church DM, Bunke B, Kunig D, Moreno-De-Luca D, Moreno-De-Luca A, Mulle JG, Warren ST, Richard G, Compton JG, Fuller AE, Gliem TJ, Huang S, Collinson MN, Beal SJ, Ackley T, Pickering DL, Golden DM, Aston E, Whitby H, Shetty S, Rossi MR, Rudd MK, South ST, Brothman AR, Sanger WG, Iyer RK, Crolla JA, Thorland EC, Aradhya S, Ledbetter DH, Martin CL. An evidence-based approach to establish the functional and clinical significance of copy number variants in intellectual and developmental disabilities. *Genet Med* 2011;13:777–84.
4 Merikangas AK, Corvin AP, Gallagher L. Copy-Number variants in neurodevelopmental disorders: promises and challenges. *Trends Genet* 2009;25:536–44.
5 Wilkie AO, Buckle VJ, Harris PC, Lamb J, Barton NJ, Reeders ST, Lindenbaum RH, Nicholls RD, Barrow M, Bethlenfalvay NC, Hutz MH, Tolmie JL, Weatherall DJ, Higgs DR. Clinical features and molecular analysis of the alpha thalassemia/mental retardation syndromes. I. cases due to deletions involving chromosome band 16p13.3. *Am J Hum Genet* 1990;46:1112–26.
6 Harteveld CL, Higgs DR. Alpha-Thalassaemia. *Orphanet J Rare Dis* 2010;5:13.
7 Buckle VJ, Rack K. Fluorescent in situ hybridisation. In: Davies KE, ed. *Human genetic disease analysis: a practical approach*. Oxford: Oxford University Press, 1993: 59–80.
8 Knight SJL, Horsley SW, Regan R, Lawrie NM, Maher EJ, Cardy DLN, Flint J, Kearney L. Development and clinical application of an innovative fluorescence in situ hybridization technique which detects submicroscopic rearrangements involving telomeres. *Eur J Hum Genet* 1997;5:1–8.
9 Horsley SW, Daniels RJ, Anguita E, Raynham HA, Peden JF, Villegas A, Vickers MA, Green S, Waye JS, Chui DHK, Ayyub H, MacCarthy AB, Buckle VJ, Gibbons RJ, Kearney L, Higgs DR. Monosomy for the most telomeric, gene-rich region of the short arm of human chromosome 16 causes minimal phenotypic effects. *Eur J Hum Genet* 2001;9:217–25.
10 Zeitlin HC, Weatherall DJ. Selective expression within the human alpha globin gene complex following chromosome-dependent transfer into diploid mouse erythroleukaemia cells. *Mol Biol Med* 1983;1:489–500.
11 Fu W, O'Connor TD, Jun G, Kang HM, Abecasis G, Leal SM, Gabriel S, Rieder MJ, Altshuler D, Shendure J, Nickerson DA, Bamshad MJ, Akey JM, NHLBI Exome Sequencing Project. Analysis of 6,515 exomes reveals the recent origin of most human protein-coding variants. *Nature* 2013;493:216–20.
12 Wang K, Li M, Hakonarson H. ANNOVAR: functional annotation of genetic variants from high-throughput sequencing data. *Nucleic Acids Res* 2010;38:e164.
13 European Polycystic Kidney Disease Consortium. The polycystic kidney disease 1 gene encodes a 14 KB transcript and lies within a duplicated region on chromosome 16. The European polycystic kidney disease Consortium. *Cell* 1994;77:881–94.
14 Lupiáñez DG, Kraft K, Heinrich V, Krawitz P, Brancati F, Klopocki E, Horn D, Kayserili H, Opitz JM, Laxova R, Santos-Simarro F, Gilbert-Dussardier B, Wittler L, Borschiwer M, Haas SA, Osterwalder M, Franke M, Timmermann B, Hecht J, Spielmann M, Visel A, Mundlos S. Disruptions of topological chromatin domains cause pathogenic rewiring of gene-enhancer interactions. *Cell* 2015;161:1012–25.
15 Hay D, Hughes JR, Babbs C, Davies JOJ, Graham BJ, Hanssen LLP, Kassouf MT, Oudelaar AM, Sharpe JA, Suciu MC, Telenius J, Williams R, Rode C, Li P-S, Pennacchio LA, Sloane-Stanley JA, Ayyub H, Butler S, Sauka-Spengler T, Gibbons RJ, Smith AJH, Wood WG, Higgs DR. Genetic dissection of the α-globin super-enhancer in vivo. *Nat Genet* 2016;48:895–903.
16 Szalaj P, Plewczynski D. Three-dimensional organization and dynamics of the genome. *Cell Biol Toxicol* 2018;34:381–404.
17 El-Brolosy MA, Stainier DYR. Genetic compensation: a phenomenon in search of mechanisms. *PLoS Genet* 2017;13:e1006780.
18 Harteveld CL, Kriek M, Bijlsma EK, Erjavec Z, Balak D, Phylipsen M, Voskamp A, Capua Edi, White SJ, Giordano PC. Refinement of the genetic cause of ATR-16. *Hum Genet* 2007;122:283–92.
19 Pfeifer D, Poulat F, Holinski-Feder E, Kooy F, Scherer G. The Sox8 gene is located within 700 kb of the tip of chromosome 16p and is deleted in a patient with ATR-16 syndrome. *Genomics* 2000;63:108–16.
20 Bezerra MACB, Araujo AS, Phylipsen M, Balak D, Kimura EM, Oliveira DM, Costa FF, Sonati MF, Harteveld CL. The deletion of *SOX8* is not associated with ATR-16 in an HbH family from Brazil. *Br J Haematol* 2008;142:324–6.
21 The Autism Genome Project Consortium. Mapping autism risk loci using genetic linkage and chromosomal rearrangements. *Nat Genet* 2007;39:319–28.
22 Volkmar FR, Lord C, Bailey A, Schultz RT, Klin A. Autism and pervasive developmental disorders. *J Child Psychol & Psychiat* 2004;45:135–70.
23 Kirov G, Gumus D, Chen W, Norton N, Georgieva L, Sari M, O'Donovan MC, Erdogan F, Owen MJ, Ropers H-H, Ullmann R. Comparative genome hybridization suggests a role for NRXN1 and APBA2 in schizophrenia. *Hum Mol Genet* 2008;17:458–65.
24 Heireman L, Luyckx A, Schynkel KD, Dheedene A, Delaunoy M, Adam A-S, Gulbis B, Dierick J. Detection of a large novel α-thalassemia deletion in an autochthonous Belgian family. *Hemoglobin* 2019;43:112–5.
25 Timberlake AT, Choi J, Zaidi S, Lu Q, Nelson-Williams C, Brooks ED, Bilguvar K, Tikhonova I, Mane S, Yang JF, Sawh-Martinez R, Persing S, Zellner EG, Loring E, Chuang C, Galm A, Hashim PW, Steinbacher DM, DiLuna ML, Duncan CC, Pelphrey KA, Zhao H, Persing JA, Lifton RP. Two locus inheritance of non-syndromic midline craniosynostosis via rare *SMAD6* and common *BMP2* alleles. *Elife* 2016;5. doi:10.7554/eLife.20125. [Epub ahead of print:
26 Luyckx I, MacCarrick G, Kempers M, Meester J, Geryl C, Rombouts O, Peeters N, Claes C, Boeckx N, Sakalihasan N, Jacquinet A, Hoischen A, Vandeweyer G, Van Lent S, Saenen J, Van Craenenbroeck E, Timmermans J, Duijnhouwer A, Dietz H, Van Laer L, Loeys B, Verstraeten A. Confirmation of the role of pathogenic Smad6 variants in bicuspid aortic valve-related aortopathy. *Eur J Hum Genet* 2019;27:1044–53.
27 Niemi MEK, Martin HC, Rice DL, Gallone G, Gordon S, Kelemen M, McAloney K, McRae J, Radford EJ, Yu S, Gecz J, Martin NG, Wright CF, Fitzpatrick DR, Firth HV, Hurles ME, Barrett JC. Common genetic variants contribute to risk of rare severe neurodevelopmental disorders. *Nature* 2018;562:268–71.
28 Scheps KG, Francipane L, Nevado J, Basack N, Attie M, Bergonzi MF, Cerrone GE, Lapunzina P, Varela V. Multiple copy number variants in a pediatric patient with Hb H disease and intellectual disability. *Am J Med Genet A* 2016;170:986–91.
29 Robin JD, Ludlow AT, Batten K, Magdinier F, Stadler G, Wagner KR, Shay JW, Wright WE. Telomere position effect: regulation of gene expression with progressive telomere shortening over long distances. *Genes Dev* 2014;28:2464–76.
30 Bystricky K, Laroche T, van Houwe G, Blaszczyk M, Gasser SM. Chromosome looping in yeast: telomere pairing and coordinated movement reflect anchoring efficiency and territorial organization. *J Cell Biol* 2005;168:375–87.
31 Quadrifoglio M, Faletra F, Bussani R, Pecile V, Zennaro F, Grasso A, Zandonà L, Alberico S, Stampalija T. A case of prenatal neurocytoma associated with ATR-16 syndrome. *J Ultrasound Med* 2016;35:1359–61.
32 Ballif BC, Sulpizio SG, Lloyd RM, Minier SL, Theisen A, Bejjani BA, Shaffer LG. The clinical utility of enhanced subtelomeric coverage in array CGH. *Am J Med Genet A* 2007;143A:1850–7.

J Med Genet: first published as 10.1136/jmedgenet-2019-106528 on 31 January 2020. Downloaded from http://jmg.bmj.com/ on April 23, 2024 by guest. Protected by copyright.

33 Flint J, Craddock CF, Villegas A, Bentley DP, Williams HJ, Galanello R, Cao A, Wood WG, Ayyub H, Higgs DR. Healing of broken human chromosomes by the addition of telomeric repeats. *Am J Hum Genet* 1994;55:505–12.
34 Gu W, Zhang F, Lupski JR. Mechanisms for human genomic rearrangements. *Pathogenetics* 2008;1:4.
35 Stankiewicz P, Lupski JR. Genome architecture, rearrangements and genomic disorders. *Trends Genet* 2002;18:74–82.
36 Hannes F, Houdt JV, Quarrell OW, Poot M, Hochstenbach R, Fryns J-P, Vermeesch JR. Telomere healing following DNA polymerase arrest-induced breakages is likely the main mechanism generating chromosome 4p terminal deletions. *Hum Mutat* 2010;31:1343–51.
37 Yang D, Xiong Y, Kim H, He Q, Li Y, Chen R, Songyang Z. Human telomeric proteins occupy selective interstitial sites. *Cell Res* 2011;21:1013–27.
38 Stadler G, Rahimov F, King OD, Chen JCJ, Robin JD, Wagner KR, Shay JW, Emerson CP, Wright WE. Telomere position effect regulates DUX4 in human facioscapulohumeral muscular dystrophy. *Nat Struct Mol Biol* 2013;20:671–8.
39 Franke M, Ibrahim DM, Andrey G, Schwarzer W, Heinrich V, Schöpflin R, Kraft K, Kempfer R, Jerković I, Chan W-L, Spielmann M, Timmermann B, Wittler L, Kurth I, Cambiaso P, Zuffardi O, Houge G, Lambie L, Brancati F, Pombo A, Vingron M, Spitz F, Mundlos S. Formation of new chromatin domains determines pathogenicity of genomic duplications. *Nature* 2016;538:265–9.
40 Rao SSP, Huntley MH, Durand NC, Stamenova EK, Bochkov ID, Robinson JT, Sanborn AL, Machol I, Omer AD, Lander ES, Aiden EL. A 3D map of the human genome at kilobase resolution reveals principles of chromatin looping. *Cell* 2014;159:1665–80.
41 Coelho A, Picanço I, Seuanes F, Seixas MT, Faustino P. Novel large deletions in the human alpha-globin gene cluster: Clarifying the HS-40 long-range regulatory role in the native chromosome environment. *Blood Cells Mol Dis* 2010;45:147–53.
42 Harteveld CL, Voskamp A, Phylipsen M, Akkermans N, den Dunnen JT, White SJ, Giordano PC. Nine unknown rearrangements in 16p13.3 and 11p15.4 causing alpha- and beta-thalassaemia characterised by high resolution multiplex ligation-dependent probe amplification. *J Med Genet* 2005;42:922–31.
43 Daniels RJ, Peden JF, Lloyd C, Horsley SW, Clark K, Tufarelli C, Kearney L, Buckle VJ, Doggett NA, Flint J, Sequence HDR. Sequence, structure and pathology of the fully annotated terminal 2 Mb of the short arm of human chromosome 16. *Hum Mol Genet* 2001;10:339–52.
44 Gibson WT, Harvard C, Qiao Y, Somerville MJ, Lewis MES, Rajcan-Separovic E. Phenotype–genotype characterization of alpha-thalassemia mental retardation syndrome due to isolated monosomy of 16p13.3. *Am J Med Genet A* 2008;146A:225–32.
45 Phylipsen M, Chaibunruang A, Vogelaar IP, Balak JRA, Schaap RAC, Ariyurek Y, Fucharoen S, den Dunnen JT, Giordano PC, Bakker E, Harteveld CL. Fine-tiling array CGH to improve diagnostics for α- and β-thalassemia rearrangements. *Hum Mutat* 2012;33:272–80.
46 Lamb J, Harris PC, Wilkie AO, Wood WG, Dauwerse JG, Higgs DR. De novo truncation of chromosome 16p and healing with (TTAGGG)n in the alpha-thalassemia/mental retardation syndrome (ATR-16). *Am J Hum Genet* 1993;52:668–76.
47 Felice AE, Cleek MP, McKie K, McKie V, Huisman TH. The rare alpha-thalassemia-1 of blacks is a zeta alpha-thalassemia-1 associated with deletion of all alpha- and zeta-globin genes. *Blood* 1984;63:1253–7.
48 Fei YJ, Liu JC, Walker EL, Huisman TH. A new gene deletion involving the alpha 2-, alpha 1-, and theta 1-globin genes in a black family with Hb H disease. *Am J Hematol* 1992;39:299–303.
49 Lindor NM, Valdes MG, Wick M, Thibodeau SN, Jalal S. De novo 16p deletion: ATR-16 syndrome. *Am J Med Genet* 1997;72:451–4.

J Med Genet: first published as 10.1136/jmedgenet-2019-106528 on 31 January 2020. Downloaded from http://jmg.bmj.com/ on April 23, 2024 by guest. Protected by copyright.

Supplementary Information:

Case Reports

Female JT had microcytic anaemia but was otherwise normal. She was found to have an interstitial deletion of 267.4 kb that arose de novo on the maternal chromosome and the breakpoint was mapped by FISH and Southern blotting before being characterised at the sequence level by inverse PCR and found to have occurred within an Alu repetitive element (Horsley et al., 2001).

Female OY had microcytic anaemia but was otherwise normal. Results of fluorescence *in situ* hybridisation (FISH) show she has a deletion on the paternal chromosome 16 which arose *de novo* and that the breakpoint lies within cosmid 419C1 (Supplementary Table 1), revealing a truncation of ~308 kb. The breakpoint was refined by Southern blotting and identified by cloning and DNA sequencing of telomere-anchored amplification products. DNA sequence analysis shows telomeric repeats directly joined to the unique sequence (Figure 1). There is a 3 bp ambiguity, suggesting a minimal telomerase-binding site contributed to the stabilisation of this breakpoint by addition of a telomere. The last unique base is position 308,543 bp, interrupting the second intron of *AXIN1* (Figure 2). There are no repeats within 300 bp either side of the break.

Female patient CS was initially referred at the age of 2 months because of an abnormal head shape, which was shown by three dimensional computed tomography scan of the skull to be associated with bicoronal craniosynostosis. Screening known craniosynostosis-associated genes by DNA sequencing and for copy number variation by MLPA revealed no pathogenic variants. However, genome-wide microarray analysis (Agilent ISCA 60K oligoarray) revealed a ~290 kb deletion, affecting 15 coding genes, between 36,766 bp and 328,247 bp on chromosome 16, which was found to have been inherited from the patient's unaffected father. CS was reported to have normal developmental milestones at the age of 8 months and there were no concerns raised about her eating, sleeping or any aspect of her behaviour. She attended normal preschool from the age of four and on follow-up at the age of 5 years there were no reported concerns about her development. Although the craniosynostosis in this patient is likely to be genetic in origin, given the absence of this phenotype in all other cases with 16p13.3 deletions, including her transmitting father, it is unlikely to be related to her chromosome 16

deletion; neither the patient nor her father have any abnormalities indicative of broader ATR-16 syndrome.

Male BF was reported found to have α-thal trait and his deletion was identified by MLPA and characterised by low coverage WGS to be between 166,680 bp and 342,681 bp (Heireman et al., 2019). This patient was one of six confirmed deletion carriers in this family, one of whom (Patient 6) has symptoms consistent with ATR-16 syndrome, however, this did not segregate with the deletion and the authors conclude this to be unrelated to the chromosome 16 deletion as the remaining carriers exhibited only α-thalassemia.

Female CV (patient F in Coelho et al., 2010) presented with microcytic anaemia suspected of being α-thalassemia and was found by MLPA to have a deletion of ~177 kb including the entire α-globin locus and extending beyond the TMEM8A gene. This individual had no abnormalities beyond the α-thalassemia.

Individual AB was referred with a suspected haemoglobinopathy and was found by MLPA to harbour a terminal chromosome 16p deletion of with a maximum extent of 400 kb (Harteveld et al., 2005). This patient was not reported to have any abnormalities beyond α-thalassemia.

Male LA presented with α-thalassemia with language delay and hypotonia. However, he has no developmental delay or skeletal abnormalities. This patient also has a brother who harbours the same deletion and has significant developmental delay including speech delay, reduced attention span, behavioural problems and seizures. Microarray analysis revealed this patient to have an interstitial deletion of ~408 kb.

Individuals TY(MI) and TY(Mi) are father and daughter respectively and have no abnormalities apart from α-thalassemia. FISH suggests the 16p breakpoint lies within cosmid 338H10 (Supplementary Table 1), indicating a truncation of ~600 kb. The deletion was refined by Southern blotting and identified by Sanger sequencing of cloned telomere-anchored amplification products to be at 596,289 bp (Figure 1), in the second intron of *RAB40C* (Figure 2). The presence of telomeric repeats added directly to the breakpoint shows telomere mediated healing, however, there is no overlap at the breakpoint junction. The break occurs at a position 16 bp within the third iteration (of 6.5) of a 66 bp tandem repeat sequence. The repeat contains 2 ORFs, one similar to alpha collagen the other similar to AHA1, activator of heat shock 90kDa protein ATPase homolog 2 (yeast). These repeats are not present elsewhere in the genome. There is a long tandem repeat similar to MLT1E1 or

MLT1E2 located 221 bp centromeric of the breakpoint and 366 bp telomeric of the break there is an LTR variant (L1ME3A). It is possible that the presence of these repeated sequences contributed to the chromosomal leading to this deletion.

Female YA had speech delay (no words by the age of 2 years) and her development was delayed by 6-12 months. She has some facial dysmorphism with mild frontal bossing, prominent eyes, flat nasal bridge, low set ears and macroglossia. She also had short stature, inverted nipples, supernumerary nipples and a bifid uvula. YA showed evidence of microcytic anaemia and because of this she was referred to our laboratory for genetic testing. FISH studies showed a deletion at the tip of chromosome 16 with breakpoint at ~750 kb (between cosmid clones C444G9 and C335H7 – Supplementary Table 1). The maternal chromosomes appeared normal, however, as the father was lost to follow-up parental origin could not be established. High-resolution microarray refined the breakpoint to ~747,840 bp (Supplementary Figure 3) ~5 kb 5' of the *MSLN* gene in an area containing L1MB7 and L1MB8 LINE repeats and AluSx and AluSq/x SINE repeats that are likely to have contributed to the rearrangement.

Female patient BA was previously reported (Daniels et al., 2001) to have no physical abnormalities but does have speech delay and a lack of spatial awareness and visual memory. Cloning and DNA sequencing of telomere-anchored amplification products shows the breakpoint to be at 762,272 bp (Figure 1) disrupting the *MSLNL* gene by removing the last four exons. The break appears to be have been healed by telomerase as TAACCC repeats are immediately adjacent to the breakpoint and there is a potential 1 bp overlap. The break occurred at a position 65 bp into an AluY repeat, which may have contributed to an instability in this region.

Male patient GZ had surgery to repair pyloric stenosis shortly after birth and had persistent microcytic anaemia, however, there was no developmental delay nor any other abnormalities related to ATR-16 syndrome (Harteveld et al., 2007). MLPA revealed this patient to have a terminal deletion with a maximum extent of 900,907 bp with the breakpoint disrupting the *LMF1* gene.

Individuals TN(Pe) and TN(Al) are brothers and TN(Pa) is their mother. All three affected family members suffered from mild intellectual delay and developmental delay (6 months to 1 year delayed speech and walking). This family have been previously reported (Daniels et al., 2001), however, in this work we have identified the breakpoint using monochromosomal somatic cell hybrid mapping

followed by DNA sequencing of telomere anchored amplification products to reveal the lesion to be at 966,713 bp, (Figure 1). We also show that this deletion arose *de novo* on the maternal allele in Tn(Pa). The break interrupts the third exon of the *LMF1* gene (Figure 2) with no repeats in the vicinity. The break appears to have been healed by telomerase as there are TAACCC repeats joined with 3 bp of overlap suggesting a minimal telomerase recognition site which facilitated the telomere mediated healing (Figure 1). Whole genome sequencing of all three affected individuals revealed no rare coding polymorphisms on the extant chromosome 16 allele. However, all three affected individuals harboured a R12X variant in *SMAD6*, a gene which has previously been associated with developmental delay with variable penetrance.

The five individuals designated with the prefix F are from a Brazilian family reported in 2008 who were found to harbour a deletion of ~931 kb identified by MLPA (Bezerra et al., 2008). This deletion disrupted the *SOX8* gene and none of the family members showed any of the broader phenotypic abnormalities of ATR-16 syndrome. This was the first reported case that showed haplo-insufficiency for *SOX8* in humans doesn't cause phenotypic abnormalities.

Female patient GIB was initially presented with a mild hypochromic microcytic anaemia and the presence of HbH inclusions (Gibson et al., 2008). Developmental delay was diagnosed at the age of 2 years, however, she did not have any dysmorphic features at this stage. By the age of 6 years craniofacial abnormalities were reported including a high forehead, flattening of the maxilla and a high nasal root and bridge together with up-slanting palpebral fissures. Intellectual abilities were reported as being around the 4th centile. Together these features are all typical of the broader ATR-16 phenotype. Microarray and FISH analyses showed a *de novo* interstitial deletion of ~900 kb in the subtelomeric region of chromosome 16p13.3 likely to be responsible for causing the abnormalities present in patient Gib.

Patient SH(Pa) exhibited motor delay throughout childhood, he had an IQ of 48 when tested and has facial dysmorphism including micrognathia, maxillary hypoplasia and a high, arched palate. He also has skeletal abnormalities including clinodactyly, tapering fingers with narrow nails, a short 4th metacarpal, intoed gait, pes planus and genu valgus. Other abnormalities include crypto-orchidism and a hypoplastic scrotum. Monosomy for 16p13.3 was identified by FISH, with the break being found to be between clones C349E11 and C344F5, (Supplementary Table 1) and subsequently refined by Southern blotting and inverse PCR to obtain the breakpoint

sequence. This revealed the rearrangement to be an interstitial AluY mediated 1,098,548 bp deletion (between ~34037 bp to ~1132584 bp), the breakpoints of which do not directly disrupt a gene (Figure 2). Because this deletion is mediated by Alu repeats there is 38 bp of overlapping sequence, making it is impossible to define the precise breakpoint (Figure 1). However, minor variations in the repeat sequence allow the last unique bases on either side of the deletion to be determined (asterisks in Figure 1). The telomeric break removes the most distal gene on 16p13.3 (*POLR3K*) and the proximal break occurs between the *C1QTNF8* and *CACNA1H* genes (Figure 3). Interestingly this breakpoint appears to be mediated by the same AluY element associated with the interstitial deletion in JT (see Figure 2) suggesting this locus may be particularly prone to rearrangement.

Male NL was diagnosed with α-thalassemia at the age of 9 years, there were no signs of mental retardation, he followed a normal school education and had normal developmental milestones. At present he is 19 years of age and studies law and plays soccer in his local team. MLPA and subsequently microarray analysis (Phylipsen et al., 2012) showed this patient to have a distal deletion of ~1.14 Mb with the breakpoint falling between *C1QTNF8* and *CACNA1H* (Figure 2). This deletion is slightly larger than that identified in family SH, surprisingly, however, it is not associated with any abnormalities apart from α-thalassemia.

A large terminal deletion of at least 1 Mb was identified in case DO by Wilkie and colleagues (Wilkie et al, 1990) using Southern blotting. This patient has craniofacial abnormalities including hypertelorism, a prominent nasal bridge, a high palate with crowded upper teeth and a small chin. Skeletal examination was normal (apart from short stature) but she had a marked speech delay, having a very limited vocabulary at the age of five years.

Male patient CJ had a birth weight of 3.2 kg and was initially referred for genetic testing because of developmental delay, speech delay and slow cognitive, social and motor development at 14 months of age. He exhibited a range of dysmorphic features including a high, broad forehead, a long and flat midface, a high narrow palette, retrognathia, micrognathia and downturned palpebral fissures. Skeletal abnormalities included bilateral hallux valgus and bilateral clinodactyly of the 5th finger. He had a systolic ejection heart murmur. Because CJ was found to have microcytic anaemia in combination with these abnormalities a possible diagnosis of ATR-16 was pursued. FISH studies revealed an interstitial deletion of the terminal region of chromosome 16 shown by absence of probes intervening the telomeric cosmid CRA36 and proximal

cosmid C399E4 (Supplementary Table 1). The deletion in this patient was refined by high-resolution microarray, which revealed it to be between ~120,000 bp and ~1,357,000 bp on chromosome 16 (Supplementary Figure 3) giving a total deletion size of ~1.15 Mb (Figure 2).

Female patient MY had a birth weight of 2.7 kg, she initially fed poorly although her health improved following surgical repair of an atrial septal defect. MY's heart defect is unlikely to be linked to the ATR-16 syndrome as her sister also had an atrial septal defect yet did not inherit monosomy for chromosome 16p13.3, although this cannot be excluded. MY also has plageocephaly and mild telecanthus and hypertelorism. She had delayed speech and mild delay to her physical development (the patient walked at 18 months of age). Results of FISH with 16p cosmids suggest the breakpoint lies between cosmids 399E4 and 312E8 (Supplementary Table 1), indicating terminal deletion of approximately 1.4 Mb. Southern blotting followed by cloning and DNA sequencing of telomere-anchored amplification products showed the break occurred at 1,408,561 bp (Figure 1), between two tandem AluSx SINE repeats, flanked by the *C16orf91* and *UNKL* genes (Figure 2). There is a rearrangement at the breakpoint with complex deletion of part of the AluSx repeat (Supplementary Figure 2). Telomeric sequence is joined directly to the breakpoint with a 2 bp overlap, suggesting telomerase mediated healing (Figure 1).

Female BAR was diagnosed with α-thalassemia by the identification of HbH inclusions at the age of 7 years. She was found to have inherited the –α3.7 deletion from her mother on one allele and MLPA and subsequently microarray analysis revealed an interstitial deletion from ~0-23,949 bp to ~1,461,124 bp had arisen *de novo* on the other allele (Figure2 and Supp. Fig 3). BAR had no phenotypic abnormalities beyond her α-thalassemia.

Male patient SCH was referred with at the age of 8 years with HbH disease to a normal mother and a father a haematological profile with a+ -thalassemia (Scheps et al., 2016). In his neonatal period, he required hospitalisation for respiratory distress and hypotonia. He also showed developmental delay and other dysmorphic craniofacial features and abnormalities of the hands and lower limbs (Scheps et al., 2016). FISH, SNP-array and MLPA revealed this patient to have an interstitial deletion of ~1.2 Mb.

Male patient PV had developmental delay at the age of 2, at the age of 11 he was noted to have mildy dysnmorphic craniofacial features, his truck showed pectus

excavatum and hyperlaxity of his joints was observed (Harteveld et al., 2007). MLPA revealed this patient to have a terminal deletion with a maximum extent of ~1.7 Mb (Harteveld et al., 2007).

Female patient FT was referred at the age of 30 years because of mild microcytic hypochromic anaemia. In infancy it was noted she had a developmental delay (Harteveld et al., 2007). At the age of 31 examination revealed craniofacial abnormalities and abnormalities of the hands and feet including clinodactly and lateral deviation. MLPA revealed a large deletion of 16p13.3 with a maximum extent of ~1.9 Mb.

Male patient BO had a small head, mild ptosis, a small mouth and a long filtrum and bilateral talipes equinovarus (reviewed in Wilkie et al., 1990). The breakpoint was refined by Wilkie and colleagues and subsequently identified as a atr terminal deletion of ~1.9 Mb (Lamb et al., 1993).

Male patient HN was reported by Harteveld and colleagues (Harteveld et al., 2007). At the age of 10 months he had delayed motor development and hypotonia. Speech delay was reported at the age of 30 months and at 3 years he was found to have an active language delay. He also had typical facial features associated with ATR-16 including downslanting palpebral fissures, mild hyperterlorism, abnormal ears. His skeletal defects were mild with only a club foot (left) and a flat foot (right) reported). MLPA revealed this patient to have a large deletion of a 1.9 Mb.

The phenotypic abnormalities of female patient IM have previously been reported (Daniels et al., 2001; Fei et al., 1992; Felice et al., 1984). Briefly, she was found to have microcytic anaemic at the age of 5 months, her growth was slow and motor retardation was noted by the age of 1 year. IM was later reported to have to suffer developmental delay (behaving like a 5 year old at the age of 8), however, her language and adaptive development were considered normal. IM has mild facial dysmorphism (tall forehead and macrodontia) and bilateral clubbed feet that were surgically corrected in early childhood. Previous studies performed Southern blotting (Fei et al., 1992) and FISH (Daniels et al., 2001) to refine the deletion, here we conduct high-resolution microarrays that reveal a large terminal deletion of chromosome 16 with the breakpoint at ~2,011,646 bp. The relatively mild phenotypic abnormalities seen in this patient are surprising given the relatively large deletion of chromosome 16 identified.

Female patient LIN had expressive speech delay and developmental delay that has been described previously (Lindor et al., 1997). She has a degree of facial

dysmorphism including a tall, broad forehead and a broad nasal root and midface retrusion. Previous FISH studies identified a terminal deletion of chromosome 16 with the breakpoint ~ 2 Mb from the telomere (Daniels et al., 2001). In this study we further refined the deletion using Southern blotting and identified the junction fragment by DNA sequencing of telomere anchored amplification products to be at 2,013,658 bp (Figure 1). The breakpoint is flanked by the genes *NPW* and *SLC9A3R2* (Figure 2). There is a short region of subtelomeric sequence of unspecified chromosomal origin between the break and the telomeric repeats suggesting a recombination-based mechanism may have stabilised the chromosomal breakage in this case (Figure 1). The lack of skeletal abnormalities seen in LIN is surprising given that the deletion is over 2 Mb.

Supplementary Methods

Genes and Assay Numbers Used in Quantification of Gene Expression

POLR3K (Hs00363121_m1), *C16orf33* (Hs00430677_m1), *C16orf35* custom assay (Forward; CAACGCCCTCAGCTTTGG, Reverse; GCTGGTGAGGGTCATGTCATC, Probe; CCCCAACCAGCAGC), *LUC7L* (Hs00216077_m1), *AXIN1* (Hs00394718_m1), *MRPL28* (Hs00371771_m1), *TMEM8* (Hs00430491_m1), *NME4* (Hs00359037_m1), *DECR2* (Hs00430406_m1), *Rab11FIP3* (Hs00608512_m1) *ACTB* (Hs99999903_m1). Two custom assays were obtained from Eurogentec (www.uk.eurogentec.com): *MPG* (Forward; 5'-GCATCTATTTCTCAAGCCCAAAG-3', Reverse; 5'-GGAGTTCTGTGCCATTAGGAAGTC-3', Probe; 5'-AGTTCTTCGACCAGCCGGCAGTCC-3') and C16orf9 (Forward; 5'-GGCGGCCCGTTCAAG-3', Reverse; 5'-GAGCCCACAAGAAGCACA-3', Probe; 5'-TCCCAGGGAACGCCGGTG-3'). Analysis was performed using the comparative C_T Method ($\Delta\Delta C_T$) (Livak et al., 2001). Data in Figure 3A were obtained by amplification and Sanger sequencing of informative polymorphisms from genomic DNA and cDNA.

Microarray Analysis

DNA from patient LA was tested using an 8 x 60K SurePrint G3 custom CGH + SNP microarray (Agilent) and analysed using Agilent Cytogenomics software 4.0. Genomic DNA from patients NL and BAR was analysed using a custom fine tiling array covering the alpha- and beta-globin gene clusters and surrounding areas was used (Roche NimbleGen, Madison, WI, USA). Array design was based on NCBI Build 36.1 (hg18) and used as previously described (Phylipsen et al., 2012). Genomic DNA from patients SH(Ju) and SH(Pa) was tested using CytoScan HD arrays (Affymetrix) and analysed using Karyoview software. Microarray analysis was performed with genomic DNA from patients CJ, IM and YA using the Sentrix Human CNV370 BeadChip (Illumina) and analysed using GenomeStudio software. DNA from patient CS was analysed using the Agilent ISCA (International Standards for Cytogenomic Arrays) 60K oligoarray.

Supplementary Figures

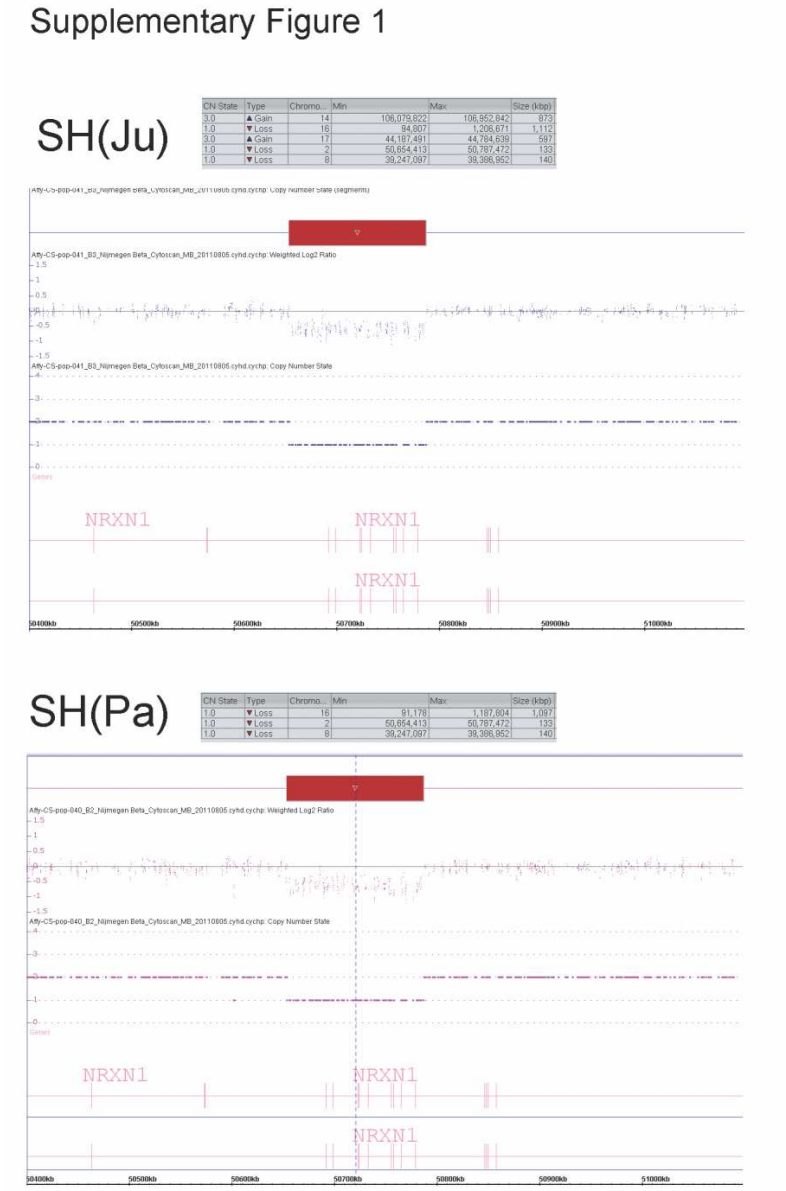

Supplementary Figure 1: Copy number variations (CNVs) identified in SH(Ju) and SH(Pa). Tables show CNVs called by Affymetrix Cytoscan software and figures below show the log2 ratio of probes and the copy number state for the chromosome 2 deletion encompassing exons 5 to 13 of *NRXN1*. Both individuals also harbour deletions of chromosomes 8 and 16. The chromosome 8 deletion disrupts the pseudogene *ADAM5* and *tMDC* encoding uncharacterised protein ENSP00000328747. The chromosome 16 deletion underlies the ATR-16 syndrome in these patients.

Supplementary Figure 2

MY breakpoint Seq:

```
AGCCTGGCCA tCATGGCGAA ACCtcacatg gtagcgggca ccaGTAATCC  50
CAGCTACTCa GGAGGCTGAG GCAGAAGAAt TGCTTGAACC CAGGAGACAA  100
GAGGTTGCAG TGAGCCAAAA TTGTGCCACT GCACTCCAGT CTGGGAGACA  150
GAGTGAGACC CTGTCTCAAA AATAAAAACA AAACAAAACA AAACAAAAAA  200
ACAAAAAACA ATCACTTAGG TAACCCAAAA TAGTGCCCAT CATTTGTGAA  250
AAGAAATACT CACTAGTatc ttgctgaaaa actcgagcca tccggaagat  300
ctggcggccg ctctccattt nagtgagtcg a
```

Genomic Chr 16:

```
gtatgaaaac aattgaccgg gcgcagtggc tcatgcctat aatcccagaa  1408510
ctttgggagg ccaaggcggg cagatcactt gaggtcagga atctgagacc  1408560
AGCCTGGCCA aCATGGCGAA ACCccgtctc tactaaaaat acaaaaatta  1408610
gacgggtgtg gcggtgcgtg cctGTAATCC CAGctaccct ggaggctgag  1408660
gcaggagagt cgcttgaacc caggaggtgg aggttgcagt gagccaagat  1408710
ggagccactg tactctagcc taggtgacag agcaagactc aatctcaaaa  1408760
aaaaaaagag aaaacaatct ggggccgggc gcggtggctc ccatctgtaa  1408810
tcccagcact gtgagaggcc gaggaggaga gatcacttga agtcaggagt  1408860
ttgagaccag cctggccaac atgccaaaag cccgtctcta ctgaaaattt  1408910
aaaaattatc cgggtgtggt ggcacaagcc tgtagttcta gCTACTCgGG  1408960
AGGCTGAGGC AGAAGAAcTG CTTGAACCCA GGAGACAAGA GGTTGCAGTG  1409010
AGCCAAAATT GTGCCACTGC ACTCCAGTCT GGGAGACAGA GTGAGACCCT  1409060
GTCTCAAAAA TAAAAACAAA ACAAAACAAA ACAAAAAAAC AAAAAACAAT  1409110
CACTTAGGTA ACCCAAAATA GTGCCCATCA TTTGTGAAAA GAAATACTCA  1409160
CTAGTtgtat tctactcaga aaatggttgc cttgcttaaa aagttttgca  1409210
gaaaactgca aaagttcctc atttctggta ctattcggta atatatatgt  1409260
aggtt
```

Side by Side alignment:

```
0000001 agcctggccatcatggcgaaacc 0000023
>>>>>>> |||||||||| |||||||||||| >>>>>>>
1408561 agcctggccaacatggcgaaacc 1408583

0000044 gtaatcccag 0000053
>>>>>>> |||||||||| >>>>>>>
1408634 gtaatcccag 1408643

0000054 ctactcaggaggctgaggcagaagaattgcttgaacccaggagacaagag 0000103
>>>>>>> |||||| |||||||||||||||||| ||||||||||||||||||||||| >>>>>>>
1408952 ctactcgggaggctgaggcagaagaactgcttgaacccaggagacaagag 1409001

0000104 gttgcagtgagccaaaattgtgccactgcactccagtctgggagacagag 0000153
>>>>>>> ||||||||||||||||||||||||||||||||||||||||||||||||| >>>>>>>
1409002 gttgcagtgagccaaaattgtgccactgcactccagtctgggagacagag 1409051

0000154 tgagaccctgtctcaaaaataaaaacaaaacaaaacaaaacaaaaaaaca 0000203
>>>>>>> ||||||||||||||||||||||||||||||||||||||||||||||||||| >>>>>>>
1409052 tgagaccctgtctcaaaaataaaaacaaaacaaaacaaaacaaaaaaaca 1409101

0000204 aaaaacaatcacttaggtaacccaaaatagtgcccatcatttgtgaaaag 0000253
>>>>>>> ||||||||||||||||||||||||||||||||||||||||||||||||||| >>>>>>>
1409102 aaaaacaatcacttaggtaacccaaaatagtgcccatcatttgtgaaaag 1409151

0000254 aaatactcactagt 0000267
>>>>>>> ||||||||||||||| >>>>>>>
1409152 aaatactcactagt 1409165
```

Supplementary Figure 2: DNA sequence of breakpoint in patient MY (upper) shown in comparison to genomic sequence with MY breakpoint sequence highlighted in blue (middle) and the side by side alignment of these sequences (lower). The breakpoint present in MY is complex and there is rearrangement of the Alu repeat associated with breakpoint.

Supplementary Figure 3

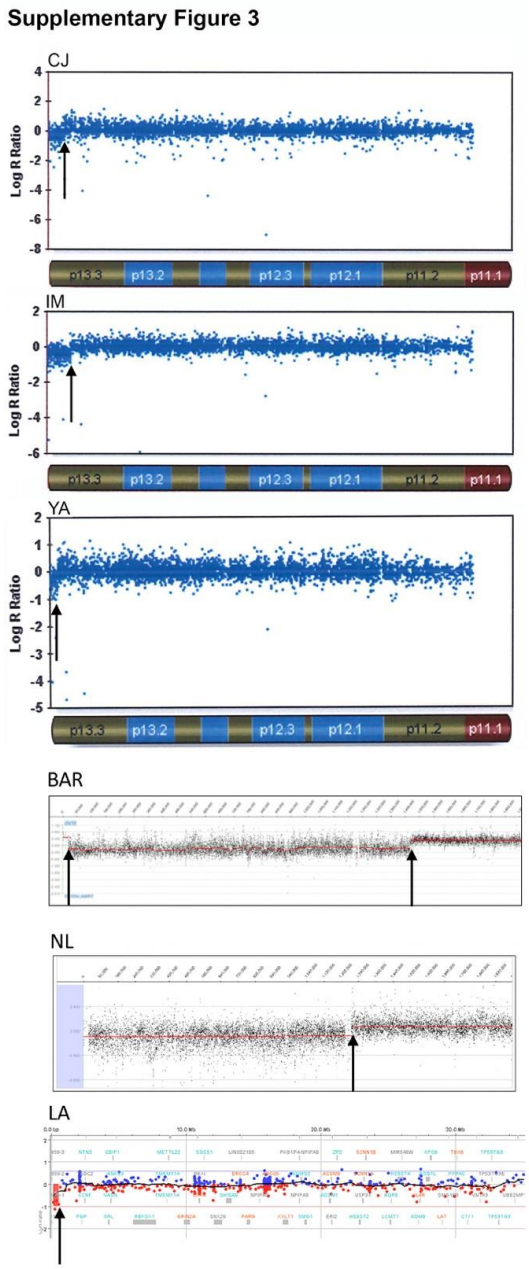

Supplementary Figure 3: Microarray data from patients CJ, IM, YA, BAR, NL and LA showing the LogR ratios of individual probes, arrows indicate loci at which analysis software identified the breakpoints.

Supplementary Figure 4

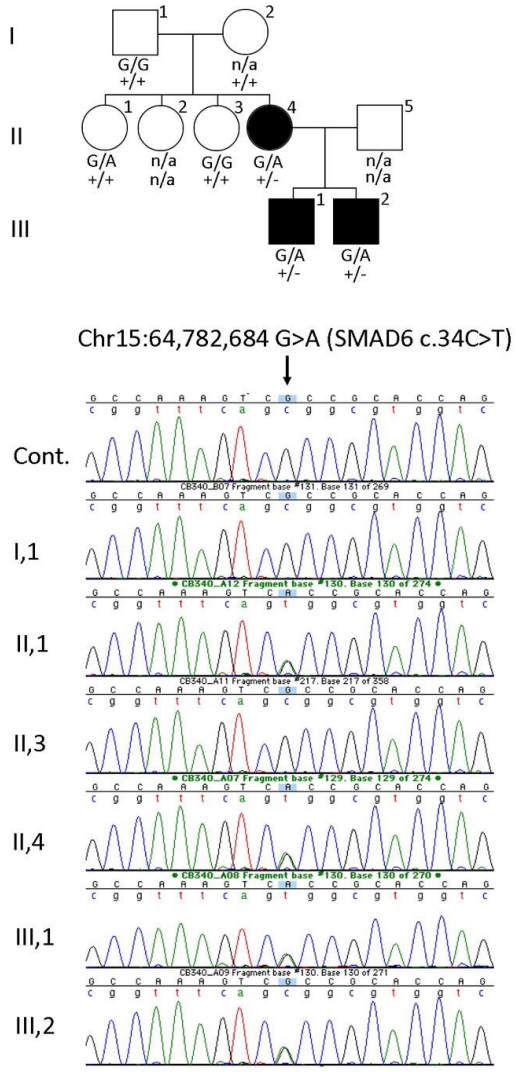

Supplementary Figure 4. Identification of SMAD6 change in Family TN. Affected family members are shown with filled symbols and unaffected individuals are represented with open symbols. Below each symbol the genotype at chr15:64,782,684 is written on the upper line, G is reference and A is the variant leading to the R12X nonsense change in *SMAD6*. The lower line of text indicates the ATR-16 deletion in this family, + indicates an intact chromosome 16 and – indicates the deleted allele. Because two siblings carry the *SMAD6* variant this is likely to have been inherited from the grandmother (I,2). Coinheritance of these variants may have led to the relatively severe ATR-16 abnormalities present in this

family. The lower part of the figure shows chromatograms for a control individual (Cont.) and family members as indicated.

Supplementary Table 1 FISH Probes

Probe	Coordinates	OY	TY	SH	MY	LIN	YA	CJ
Telomere Assay	na	N	nd	nd	N	nd	N	N
16p cosmid								
CRA36	52706-99963 bp	-						+
HSGG4	97541-111766 bp		-		-		-	
HSGG1	129137-172194 bp	-	-		-		-	-
Cos12	158777-203194 bp		-					-
C314G4	243192-285276 bp	-						
C419C1	265315-316860 bp	+/-	-					-
C338B10	297847-340834 bp	+						
C415C1	332201-381990 bp	+			-			
C356B8	485020-530746 bp	+						
C366D1	521427-565641 bp		-					
C407A10	557634-598294 bp		-					
C338H10	580029-610790 bp		+/-		-			
C398G5	594663-640361 bp	+	+					
C444G9	708336-751169 bp						-	
C335H7	737067-783265 bp						+	
C360B4	851308-895707 bp				-			
C313F9	1025418-1072203 bp	+						
C349E11	1068736-1111710 bp			-	-			-
C344F5	1122769-1160074 bp			+				
C320E12	1172104-1208298 bp							-
C399E4	1359308-1404844 bp				-			+
C312E8	1395863-1429931 bp				+			
C305C8	1461998-1505438 bp	+			+			+
C371H6	1755695-1799062 bp				+			
C439A6	1882600-1923854 bp	+						
910O19	1965888-2004708 bp					+/-		
1308N18	1996694-2036573 bp					+		
2171017	2038309-2078584 bp					+		

Presence of signals on both chromosome 16 homologues is indicated by "+", "-" indicates signal absent on one chromosome 16 homologue, "+/-" indicates weaker signal on one homologue compared to the other. The top row indicates patients who were analysed for subtelomeric rearrangements using a telomere assay (Knight et al., 1997 and Horsley et al., 2001): N, no rearrangement; nd, not done; na, not applicable.

Supplementary Table 2 Oligonucleotides used to clone breakpoints

Patient	Forward primer	Reverse primer
SH	5'-AGATACATGCTCCCAGTCTCA-3'	5'-CGTATATCTGGTCTCTATCTTC-3'
OY	5'-CAAAGCACGCATCCATAGGC-3'	5'-CCCTAACCCTGACCCTAACCC-3'
LN	5'- GCAGAGGGAGAGCAGGTCTCAG-3'	5'-CCCTAACCCTGACCCTAACCC-3'
MY	5'- CTGAAGGACTTGGCTGGTGGAT-3'	5'-CCTAACCCTGACCCTAACCC-3'
BA	5'-GAGCAAAGTACACAAACTGGGTGAC-3'	5'-CCTAACCCTGACCCTAACCC-3'
TN	5'-AACTGGCCTTGTCTGTGCCTTAAGCT-3'	5'-CCCTAACCCTGACCCTAACCC-3'
TY	5'-CCTACCACCAGCAAGAACGGA-3'	5'-CCTAACCCTGACCCTAACCC-3'

Supplementary Table 3 Deleterious Chromosome 16 Variants

Patients*	Gene#	Variant%	Identifier^	Freq$	ANNOVAR@
TN(Al, Pa, Pe)	MRPL28	H27Y	rs3194151	11%	3/6
TN (Al,Pe)	PICQ	G523S	rs7187227	14%	3/6
TN(Al) YA	PICQ	T14A	rs2071979	~49%	2/6
TN(Al, Pa,Pe) YA	POLR3K	S24A	rs3194151	100%	2/6
TN(Pa)	PDIA	T286M	rs2685127	8%	3/6
TN(Pa)	CHTF	S63F	rs2277902	5%	1/6
(Pa)	PRR25	T92S	rs1005190	41%	1/6
YA	NPRL3	R158fs	rs35963490	33%	6/6
YA	RGS11	G499A	rs9806942	15%	3/6
YA	RHOT	R425C	rs3177338	33%	3/6
YA	RHOT	R245Q	rs1139897	33%	2/6
YA	RGS11	T728C	rs739999	31%	1/6
YA	WDR90	H899Q	rs45613635	34%	1/6

*Codes for patients harbouring each of the changes listed are shown in this column. #Gene symbols are used. % Effects of variants on coding sequence. ^The unique identifier from dbSNP is listed for each variant. $ Allele frequencies as a population average, data from dbSNP. @ The pathogenicity of each variant was given a custom deleterious score based on a six-point scale, (Fu et al., 2013) calculated using output from ANNOVAR (Wang et al., 2010).

Supplementary Table 4. Shared novel variants in 3 affected members of family TN

Chr[#]	Position (bp)	Gene	Variant[$]	ANNOVAR[%]	Associated abnormalities^
1	1336598	PRAMEF27	Q144R	1/6	na
1	26671545	CRYBG2	L524fs	6/6	na
2	71190373	ATP6V1B1	R331W	4/6	Renal tubular acidosis with progressive nerve deafness.
3	141163642	ZBTB38	K804N	5/6	Potential role in human height variation (nearby GWAS association).
4	17061677	CLCN3	A290S	4/6	Loss of hippocampus in mouse KO.
5	179068881	C5orf60	splicing	6/6	na
8	125052168	FER1L6	G837D	3/6	na
11	1018248	MUC6	T1518I	2/6	Gastric cancer
11	62293804	AHNAK	F2695L	2/6	Neuroblastoma
13	103718412	SLC10A2	K63fs	6/6	Chrohn's disease, bile malabsorbtion.
14	33014538	AKAP6	L227V	5/6	na
15	66995630	SMAD6	R12X	6/6	Aortic Valve Disease, Craniosynostosis, developmental delay.
19	59010556	SLC27A5	V483M	6/6	na
20	5170758	CDS2	P406A	4/6	na

[#]Chromosome. [$]The effect of each variant on the protein is shown. [%]The custom pathogenicity score attributed to each variant (see Supp Table 3 notes). ^Annotation present in the OMIM database associated with each gene, na indicates no information in OMIM. The pathogenicity of each variant was given a custom deleterious score based on a six-point scale, (Fu et al., 2013) calculated using output from ANNOVAR (Wang et al., 2010).